Biophysical Chemistry 150 (2010) 144–156

Contents lists available at ScienceDirect

Biophysical Chemistry

journal homepage: http://www.elsevier.com/locate/biophyschem

The microstructure of the stratum corneum lipid barrier: Mid-infrared spectroscopic studies of hydrated ceramide:palmitic acid:cholesterol model systems ☆

Patrick Garidel *, Bettina Fölting, Ingrid Schaller, Andreas Kerth

Physikalische Chemie, Martin-Luther-Universität Halle-Wittenberg, Von-Danckelmann-Platz 4, D-06120 Halle/Saale, Germany

ARTICLE INFO

Article history:
Received 9 February 2010
Received in revised form 6 March 2010
Accepted 8 March 2010
Available online 30 March 2010

Keywords:
Ceramide
Skin lipids
Stratum corneum
Mid-infrared spectroscopy
Microstructure

ABSTRACT

The current mid-infrared spectroscopic study is a systematic investigation of hydrated stratum corneum lipid barrier model systems composed of an equimolar mixture of a ceramide, free palmitic acid and cholesterol. Four different ceramide molecules (CER NS, CER NP, CER NP-18:1, CER AS) were investigated with regard to their microstructure arrangement in a stratum corneum lipid barrier model system. Ceramide molecules were chosen from the sphingosine and phytosphingosine groups. The main differences in the used ceramide molecules result from their polar head group architecture as well as hydrocarbon chain properties. The mixing properties with cholesterol and palmitic acid are considered. This is feasible by using perdeuterated palmitic acid and proteated ceramides. Both molecules can be monitored separately, within the same experiment, using mid-infrared spectroscopy; no external label is necessary.

At physiological relevant temperatures, between 30 and 35 °C, orthorhombic as well as hexagonal chain packing of the ceramide molecules is observed. The formation of these chain packings are extremely dependent on lipid hydration, with a decrease in ceramide hydration favouring the formation of orthorhombic hydrocarbon chain packing, as well as temperature. The presented data suggest in specific cases phase segregation in ceramide and palmitic acid rich phases. However, other ceramides like CER NP-18:1 show a rather high miscibility with palmitic acid and cholesterol. For all investigated ternary systems, more or less mixing of palmitic acid with cholesterol is observed. The investigated stratum corneum mixtures exhibit a rich polymorphism from crystalline domains with heterogeneous lipid composition to a "fluid" homogeneous phase. Thus, a single gel phase is not evident for the presented stratum corneum model systems.

The study shows, that under skin physiological conditions (pH 5.5, hydrated, 30–35 °C) ternary systems composed of an equimolar ratio of ceramides, free palmitic acid and cholesterol may form gel-like domains delimitated by a liquid-crystalline phase boundary. The presented results support the microstructural arrangement of the stratum corneum lipids as suggested by the domain mosaic model.

1. Introduction

The skin represents the outer defence line of our body [1], with the stratum corneum being the outermost skin layer. The main functions of the stratum corneum are (i) mechanical and (ii) antimicrobial barrier function and (iii) minimising UV and IR radiation cell damages by absorbing the radiation [2]. Furthermore, the stratum corneum regulates the water homeostasis and water balance of the skin and prevents the organism from desiccation [3]. Thus, the skin's primary functions are to serve as a barrier to the entry of microbes and viruses, and to prevent water and extracellular fluid loss [4,5].

The stratum corneum represents the main skin barrier. It consists of dead cells (corneocytes), which are filled with keratin [4]. The corneocytes, which have a hexagonal-like shape of a diameter of 30–40 μm with a thickness of just 0.3–1 μm, are embedded in a multifaceted matrix of multilamellar organised lipids [4,6,7]. The cartoon often used for illustrating this stratum corneum macrostructure is the picture of a brick-and-wall-like organisation, with the corneocytes forming the bricks and the intercellular lipids representing the mortar of the wall (see discussion below).

Roughly, the stratum corneum consists of 12–15 layers of interdigitated corneocytes, which are spaced from each other by ca. 75 nm [6,8–10]. The space between the corneocytes is filled with lipids. It becomes now obvious that the corneocytes are organised in clusters of size up to 12 cells. The corneocytes are anchored in the lipid matrix by intercorneocyte lipids [11,12]. These are omega-hydroxyceramides, long molecules, which are chemically linked to the cell envelope of the corneocytes. One consequence of the presence of this lipid structure is an alignment and self-assembling of the intercellular lipids [13–17]. This intercellular lipid matrix is composed of a more or

☆ Dedicated to Prof. Dr. Alfred Blume on the occasion of his 65th birthday.

* Corresponding author.
E-mail address: Patrick.Garidel@chemie.uni-halle.de (P. Garidel).

0301-4622/$ – see front matter © 2010 Elsevier B.V. All rights reserved.
doi:10.1016/j.bpc.2010.03.008

less equimolar mixture of ceramide, long-chain free fatty acids and cholesterol [18–20]. Small amounts of cholesterol derivates like esters or sulphate are also present, but at minor amounts [4].

The chemical structure of the different ceramide molecules depends on their building blocks. Ceramides (Fig. 1) belong to the class of sphingolipids. In general a fatty acid molecule is linked via an amide bond to a sphingoid base [2]. Three types of sphingoid bases are of relevance: (i) sphingosine, (ii) phytosphingosine and (iii) 6-hydroxysphingosine [21,22]. Furthermore, three types of fatty acid structures have to be considered: (i) non-hydroxy acids, (ii) alpha-hydroxy acids and (iii) omega-hydroxy acids. These fatty acids may vary in chain length as well as in the saturation degree. Based on these combinations, the variety of ceramides is formed. Actually nine subclasses of ceramide molecules have been isolated from human skin. Initially, the different ceramides identified were classified according to their order of retention properties in the thin-layer chromatography (TLC) assay, with an increasing numbering of the identified ceramides with increasing polarity of the mobile TLC phase [8,21]. However, this classification was not appropriate. Motta et al. [23,24] have therefore proposed a new nomenclature for the classification of ceramide molecules based on their chemical architecture. They have introduced a letter code indicating the type of sphingoid base and fatty acid. According to Motta et al. [23], the last letter represents the sphingoid base (S = sphingosine, P = phytosphingosine, H = 6-hydroxysphingosine), the letter next to the last stands for the amide-linked fatty acid (N = non-hydroxy acids, A = alpha-hydroxy acids, O = omega-hydroxy acids) [21,25]. If relevant, the additional ester-linked fatty acid is indicated by a third letter (E = ester-linked fatty acid) standing first [21,26].

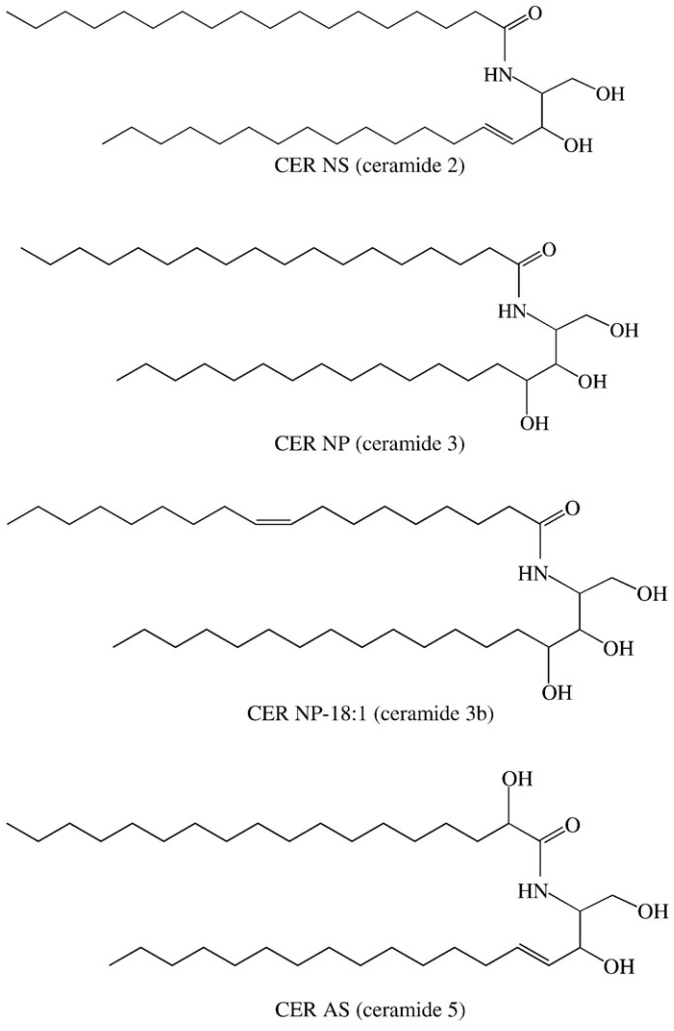

Fig. 1. Chemical structure of the used ceramides. Ceramide CER NS (ceramide 2), ceramide CER NP (ceramide 3), ceramide CER NP-18:1 (ceramide 3b), ceramide CER AS (ceramide 5). A = alpha-hydroxy fatty acid, N = non-hydroxy fatty acid, P = phytosphingosine, S = sphingosine.

It is also known that the exact composition of the stratum corneum lipid barrier strongly defines the performance of the skin properties [24,27–29]. Pilgram et al. [30] have, for example, shown that certain skin diseases are related to an aberrant stratum corneum lipid composition and organisation.

The present study investigates the microstructural organisation of hydrated ceramides in a ternary, equimolar mixture composed of free palmitic acid and cholesterol. Such ternary systems are often used as a model system for the stratum corneum lipid barrier due to its chemical defined nature [20,31–36]. However, such "primitive" model systems do not in each case completely model the stratum corneum lipid barrier properties [37,38].

To probe the lipid organisation of the ternary stratum corneum systems, Fourier transform mid-infrared (FTIR) spectroscopy is used, because FTIR allows to monitor the lipid conformation as well as the molecular organisation of membranes without the use of external probe molecules [39–42]. A main advantage using FTIR is the well known spectral–structural correlation of lipid organisation (Table 1) [39,40,43]. Furthermore, the experiments can be performed under physiological relevant conditions (impact of temperature, hydrated samples, pH of 5.5, osmolality of ca. 300 mOsmol/kg) [44–46].

The use of deuterated and proteated lipids allows the simultaneous and separate monitoring of two different lipid components in a lipid mixture and the investigation of inter- and intra-molecular interactions [47,48]. In the presented study proteated ceramide molecules were used and perdeuterated palmitic acid (pd-PA). The reason for the separate simultaneous monitoring of both lipids lies in the deuterium induced shift of C–H/C–D vibrations [49] (see Table 1).

Four different ceramides were investigated (CER NS, CER NP, CER NP-18:1, CER AS) in an equimolar ternary system.

The following aspects were considered:

(1) microstructural lipid organisation (hydrocarbon chain organisation as well as interactions in the polar interface)
(2) mixing properties with free palmitic acid and cholesterol
(3) impact of the ceramide component on the lipid organisation
(4) temperature impact on mixing and structural organisation
(5) water penetration
(6) kinetics of chain organisation.

The derived results are discussed within the frame of the domain and mosaic model.

2. Materials and methods

2.1. Materials

Bovine non-hydroxy fatty acid ceramide (CER NS), bovine hydroxy fatty acid ceramide (CER AS), cholesterol, perdeuterated palmitic acid and deuterium oxide were purchased from Sigma Aldrich (Germany) (Fig. 1). CER NS has a fatty acid chain length distribution primarily of C18:0 and C24:1, whereas CER AS has a fatty acid chain length distribution primarily of C18:0, C22:0, C24:0 and C24:1. These isolated natural ceramides are used as model systems for human ceramide NS and human ceramide AS, respectively, because they have the same chemical backbone as the human ceramides.

Ceramide CER NP [N-stearoyl phytosphingosine, (N-C18:0-PS)] and ceramide CER NP-18:1 [N-oleoyl phytosphingosine, (N-C18:1-PS)] were a gift from Cosmoferm (Delft, The Netherlands) and Goldschmidt AG (Essen, Germany).

Table 1
Assignments of the most prominent infrared absorption regions and characteristic group frequencies of skin lipids.

Frequency range/cm^{-1}	Assignment	Remarks
3300	Amide A (N–H stretching)	
ca. 3080	Amide B (N–H stretching)	
3010	=C–H stretching of alkenes	Conformational sensitive
2957	Asymmetric CH_3 stretching	
2916–2924	Asymmetric CH_2 stretching	Frequency increases when chain becomes disordered
2846–2855	Symmetric CH_2 stretching	Frequency increases when chain becomes disordered
2872	Symmetric CH_3 stretching	
2180–2195	Asymmetric CD_2 stretching	Frequency increases when chain becomes disordered
2085–2100	Symmetric CD_2 stretching	Frequency increases when chain becomes disordered
1690–1740	Ester C=O stretch	Band position sensitive to hydrogen bond formation
1650–1660	Amide I (80% C=O stretch)	Band position sensitive to hydrogen bond formation
1540–1550	Amide II (60% N–H in-plane bend, 40% C–N stretch)	Band position sensitive to hydrogen bond formation N–H → N–D exchange induces a band shift to ca. 1450 cm^{-1}
1462 and 1473	CH_2 scissoring	Orthorhombic phase doublet
1468	CH_2 scissoring	Hexagonal phase
1466	CH_2 scissoring	Disordered phase
ca. 1395	C=O stretch of COO^-	
1378	CH_3 symmetric bend	
1368	CH_2 wagging disordered	*gtg* or kink (*gtg′*) conformer sequence
1353	CH_2 wagging disordered	*gg* sequence
1341	CH_2 wagging disordered	End *gauche* conformer
1180–1350	CH_2 wagging ordered	Mode splitting in a characteristic fashion of a particular ordered chain length
1300	Amide III (40% C–N stretch, 30% N–H in-plane bend, 20% methyl-C stretch)	See amide I
1170	Ester C–O asymmetric stretch	
1092 and 1085	CD_2 scissoring	Orthorhombic phase doublet
1089	CD_2 scissoring	Hexagonal phase
1087	CD_2 scissoring	Disordered phase
728 and 720	CH_2 rocking	Orthorhombic phase doublet
721	CH_2 rocking	Hexagonal phase
720	CH_2 rocking	Disordered phase

g = *gauche*, *t* = *trans*.

The lipids were purified by re-crystallisation in a chloroform/methanol mixture. The purity of the lipid was checked before and after the experiments [50,51].

2.2. Method: Fourier transform mid-infrared spectroscopy (FTIR)

2.2.1. Instrumentation

The FTIR spectra were collected on a Bruker FTIR spectrometer Tensor 37 (Bruker-Optics, Ettlingen, Germany) equipped with a broad band MCT (Mercury Cadmium Telluride) detector. Spectra were acquired at 2 cm^{-1} resolution, 256 interferograms were collected, apodized with a triangular function and Fourier transformed after one level of zero filling [52,53]. The thermotropic phase behaviour was investigated in the temperature range between 20 and 110 °C (depending on the investigated systems) in steps of 2 K using a temperature-controlled set-up.

2.2.2. Sample preparation

A pure lipid or lipid mixture (composed of an equimolar mixture of ceramide, perdeuterated palmitic acid and cholesterol), dissolved in chloroform:methanol 2:1 (v/v), was added to AgCl windows and dried to induce the formation of a lipid film. The samples were dried under vacuum overnight as described previously [11,54]. The sample was hydrated with H_2O or D_2O, respectively, containing 10 mM phosphate buffer, 150 mM NaCl, 4 mM EDTA at pH 5.5. Two infrared windows were sandwiched and placed in a heatable cell set-up for transmission measurements. The sample cell path length was given by an 18 μm thick Teflon distance ring placed between the two infrared windows. Alternatively, a horizontal-ATR (attenuated total reflection) FTIR set-up was used (for more details see [54]).

2.2.3. Data analysis

The infrared data were analysed using the Moffat software (written at the National Research Council of Canada). Peak positions were determined by applying second derivative spectroscopy using a centre of gravity algorithm. Further spectra evaluation and manipulation were carried out using the Grams (Galactic) software as described previously [54].

3. Results

A number of infrared active vibrations are used for the elucidation of the organisation of lipids. Fig. 2 represents a mid-infrared spectrum of a dry ceramide (CER NS) film. The main vibrational modes that are used to decipher the structural organisation of the ceramides are labelled in Fig. 2. The exact positions of the different modes are listed in Table 1. From the same spectrum, information arising from (i) the hydrocarbon chain organisation as well as the (ii) interactions in the interfacial polar head group region are readily derived.

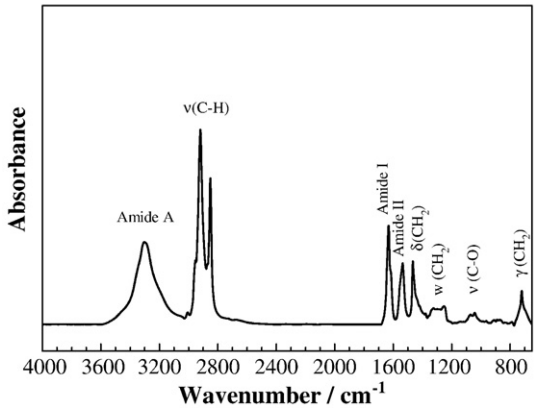

Fig. 2. A representative mid-infrared spectrum of a dry ceramide film (CER NS). The position of the major vibrational modes of the chain and head group is shown (see also Table 1). ν = stretching, δ = scissoring, w = wagging, γ = rocking mode.

3.1. Pure hydrated lipids

3.1.1. Chain vibrations

In the spectral region between 2800 and 3000 cm^{-1} the methylene stretching modes are observed as the most intensive bands (Fig. 2). The asymmetric ($\nu_{asym}(CH_2)$) and symmetric ($\nu_{sym}(CH_2)$) modes for proteated chains are found at ca. 2920 and 2850 cm^{-1}. If H (hydrogen) is substituted by D (deuterium) a shift to lower wavenumbers is induced (Table 1). The corresponding vibrations for deuterated chains arise for $\nu_{asym}(CD_2)$ at ca. 2190 and for $\nu_{sym}(CD_2)$ at ca. 2095 cm^{-1} (see for example Fig. 5A) [55]. The methylene stretching modes are extremely sensitive to temperature changes and to external conditions like the interaction of compounds (e.g. peptides) with the membrane. This sensitivity provides a quantitative indication of changes in the hydrocarbon chain packing or conformational order and alkyl chain "fluidity". For tightly packed hydrocarbon chains adopting a fully extended *all-trans* conformation the $\nu_{sym}(CH_2)$ arises at low wavenumbers of ca. 2847 cm^{-1} [41]. Increasing the temperature the amount of *gauche* conformers increases which lead to an increase of the $\nu_{sym}(CH_2)$ wavenumbers above 2853 cm^{-1} [35,41]. Therefore, this band indicator is very useful for monitoring the gel to liquid-crystalline phase transition. The same applies for $\nu_{asym}(CH_2)$ or the corresponding CD_2 vibrations (see Table 1).

Fig. 3A represents the phase transition of hydrated ceramides. The steep rise in the $\nu_{sym}(CH_2)$ versus temperature plot is defined as the main phase transition (T_m). The corresponding T_m are: T_m(CER NS) = 92 °C, T_m(CER NP) = 109 °C, T_m(CER NP-18:1) = 88 °C, T_m(CER AS) = 78 °C.

The exact T_m depends on the thermal history of the sample as well as the hydration degree or the presence of ions, especially divalent cations etc. This has been discussed extensively ([52] and references cited therein).

As can be seen from Fig. 3A sharp phase transitions, indicating the transition from a crystalline, gel-like phase to the liquid-crystalline phase are observed indicating a highly cooperative melting behaviour.

Compared to phospholipids with the same hydrocarbon chain length, the phase transition temperatures of ceramides are in general much higher. Furthermore, the absolute position of $\nu_{sym}(CH_2)$ wavenumbers, which are below 2849 cm^{-1} are indicative for the organisation of the hydrocarbon chains in a fully extended and conformationally ordered (*all-trans*) structure. For two ceramides a second, smaller transition is observed in the temperature range between 60 and 70 °C. For CER NP this transition arises at 68 °C and for CER NS at ca. 66 °C. This transition is related to a solid–solid transition (see also discussion below).

The analysis of the infrared spectrum also allows the determination of the chain packing properties [34,41,49]. To elucidate the chain packing organisation, the CH_2 scissoring ($\delta(CH_2)$) and/or CH_2 rocking ($\gamma(CH_2)$) modes are used. The position of these vibrations as well as the shape of the corresponding bands are indicative whether the alkyl chains adopt a chain packing in a hexagonal or orthorhombic perpendicular subcell lattice (Table 1 and Fig. 13E). A splitting of the scissoring or rocking band shows the formation of the hydrocarbon chains packed in an orthorhombic lattice. The positions of the $\gamma(CH_2)$ for the four hydrated ceramides as a function of temperature are shown in Fig. 3B. CER NS is packed in an orthorhombic lattice and with increasing temperature this chain packing disappears and is converted in a less tight chain packing (hexagonal). This solid–solid conversion is observed at the first transition located at ca. 66 °C. The hydrocarbon chains still adopt an *all-trans* conformation. Between 66 °C and the onset of the main phase transition temperature at ca. 88 °C hexagonal chain packing is observed. In the liquid-crystalline phase, the chains become disordered, with a strong increase of *gauche* conformers of the hydrocarbon chains (Fig. 3A).

The hydrocarbon chains of CER NP are able to adopt two packings, namely an orthorhombic and a hexagonal one, which depend on the

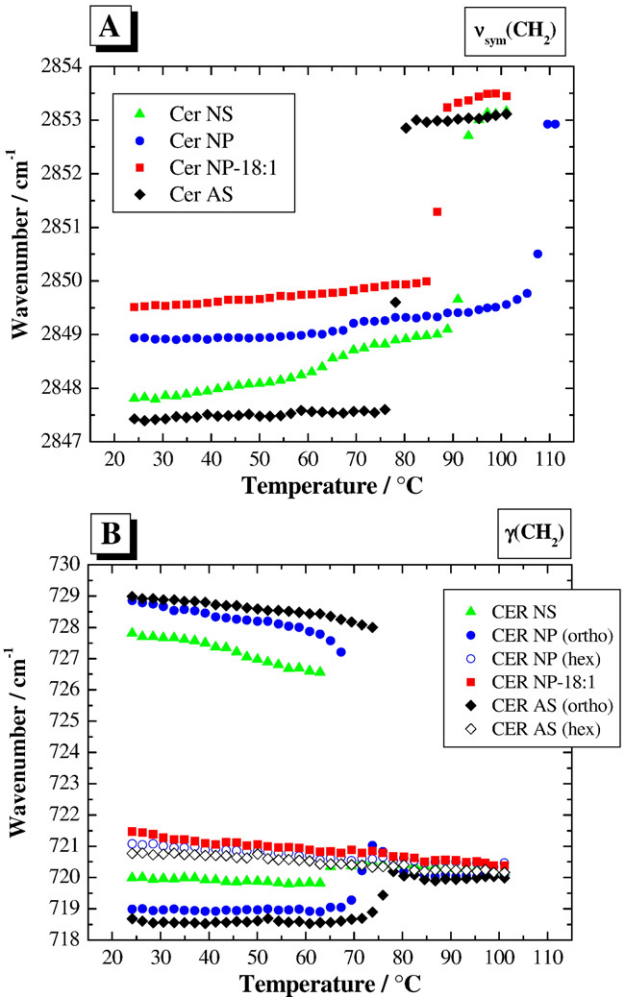

Fig. 3. (A) Temperature dependence of the symmetric CH_2 (methylene) stretching mode frequency ($\nu_{sym}(CH_2)$) of hydrated ceramides (10 mM phosphate buffer, 150 mM NaCl, 4 mM EDTA, in D_2O, pD 5.5). (B) Temperature dependence of the CH_2 (methylene) rocking mode frequency ($\gamma(CH_2)$) of hydrated ceramides (10 mM phosphate buffer, 150 mM NaCl, 4 mM EDTA, in D_2O, pD 5.5).

sample history (for more details see [52,65]). The solid–solid conversion of the orthorhombic to hexagonal chain packing is observed at ca. 68 °C. This is consistent with the changes detected for the methylene stretching vibrations (Fig. 3A). The time evolution of the formation of the orthorhombic chain packing, after the sample was heated above the gel to liquid-crystalline phase transition and cooled down to 32 °C, is represented in Fig. 4A. As can be seen, the appearance of a more or less pure orthorhombic chain packing of CER NP is achieved after a long incubation of more than 3 weeks at 32 °C. This is the case for fully hydrated CER NP. If water evaporation is induced, the re-crystallisation into an orthorhombic lattice is much faster and can be achieved within 24 h (data not shown) [56,57]. Therefore, it is very important to control water hydration, because this parameter has a strong impact on the re-organisational process of the acyl chains [52,58,59].

CER NP-18:1, which is a ceramide component used in dermatological applications [60–62], adopts only hexagonal chain packing; an orthorhombic chain packing is not observed. This is due to the presence of the double bond in the ceramide fatty acid chain compared to CER NP [52,54,63,64]. Therefore, the initial frequencies $\nu_{sym}(CH_2)$ are higher compared to the same data for CER NP (Fig. 3A).

CER AS can adopt both chain packings. The orthorhombic chain packing of CER AS undergoes directly the disordered chain organisation, because this is observed at the onset of the main phase transition

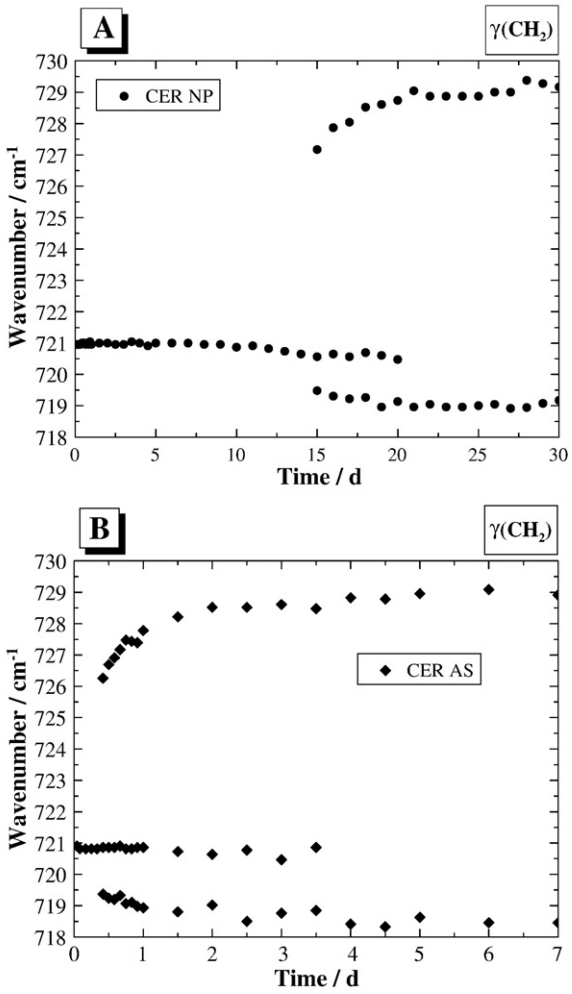

Fig. 4. Evolution of the CH_2 (methylene) rocking mode frequency ($\gamma(CH_2)$) of hydrated ceramides (10 mM phosphate buffer, 150 mM NaCl, 4 mM EDTA, in D_2O, pD 5.5) at 32 °C as a function of time (d: days). (A) CER NP. (B) CER AS.

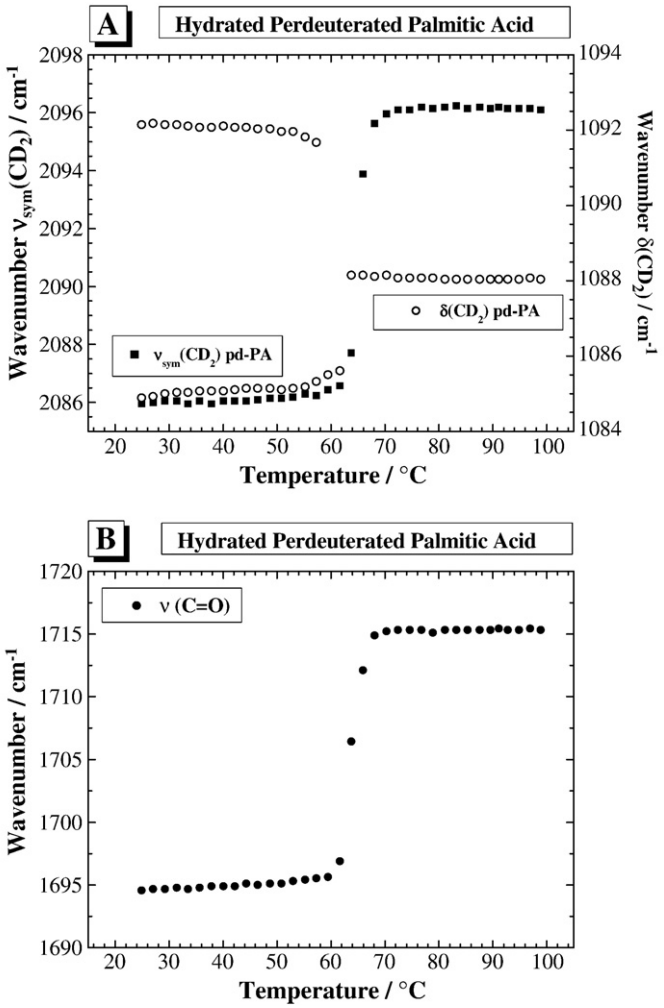

Fig. 5. Temperature dependence of (A) the symmetric CD_2 (methylene) stretching mode frequency ($\nu_{sym}(CD_2)$) and CD_2 (methylene) scissoring mode frequency ($\delta(CD_2)$) and (B) the ester ($\nu(C{=}O)$) of hydrated perdeuterated palmitic acid (pd-PA) (10 mM phosphate buffer, 150 mM NaCl, 4 mM EDTA, in D_2O, pD 5.5).

at 78 °C. A solid–solid transition is not observed. A quenching of the sample from ca. 95 °C to 32 °C induces the formation of hydrocarbon chains packed in a hexagonal subcell lattice. The re-organisation into an orthorhombic packing is much faster for CER AS compared to CER NP. For CER AS the doublet formation of the rocking $\gamma(CH_2)$ mode is observed after a storage of ca. 24 h and full re-organisation is achieved after 3.5 day storage at 32 °C under fully hydrated conditions (Fig. 4B).

In both cases (CER NP and CER AS) two different chain packings are detected [65]. However, the main phase transition is similar and independent of the original hydrocarbon chain packing (data not shown). Small differences are observed for the initial position of the methylene stretching vibration [52].

Pure, hydrated perdeuterated palmitic acid (pd-PA) at pH 5.5 shows the gel to liquid-crystalline phase transition at ca. 63 °C (Fig. 5A). The phase transition is extremely sharp, which is consistent with a highly cooperative process. The exact chain melting temperature depends on the pH of the solution as well as the presence of ions, buffer etc. The initial value at 25 °C for the $\nu_{sym}(CD_2)$ is very low with 2086 cm^{-1}, indicating a tightly packed chain arrangement. The hydrocarbon chains adopt orthorhombic chain packing below the main phase transition temperature. The collapse of the doublet to a single peak is detected at the onset of the chain melting.

3.1.2. Polar region vibrations

For elucidating the molecular organisation at the polar interface of fatty acids, the analysis of the carbonyl stretch, which is observed between 1690 and 1740 cm^{-1} is useful (Fig. 5B). With increasing temperature the carbonyl stretching mode frequency increases in a highly cooperative manner at the phase transition temperature from ca. 1695 to 1715 cm^{-1}. Low wavenumbers are characteristic for the involvement of the carbonyl group in a strong hydrogen bond network, and a weakening of these interactions is shown by an increase of the wavenumbers up to 1715 cm^{-1}.

For ceramides, the strong bands observed in the spectral regions from 1700 to 1500 cm^{-1} arise from the amide I and amide II modes (Table 1). The amide bond vibrations of these polar head group regions are extremely sensitive to the formation of a hydrogen bond network. The shape of the amide I and II bands as well as the position of the maxima of these bands are indicative for the involvement of the amide group to hydrogen bonding interactions (Fig. 6). The amide I mode arises mostly from the carbonyl stretch, whereas the amide II mode arises from a mixture of the N–H in-plane bending and C–N stretching.

Performing the experiment in D_2O instead of H_2O allows monitoring the penetration of water into the polar interface. This is due to the hydrogen–deuterium (H→D) exchange, which induces a shift of the amide II from 1545 to 1450 cm^{-1} (amide II′) Thus, the accessibility to water in the polar region is followed by a decrease of the amide II band intensity.

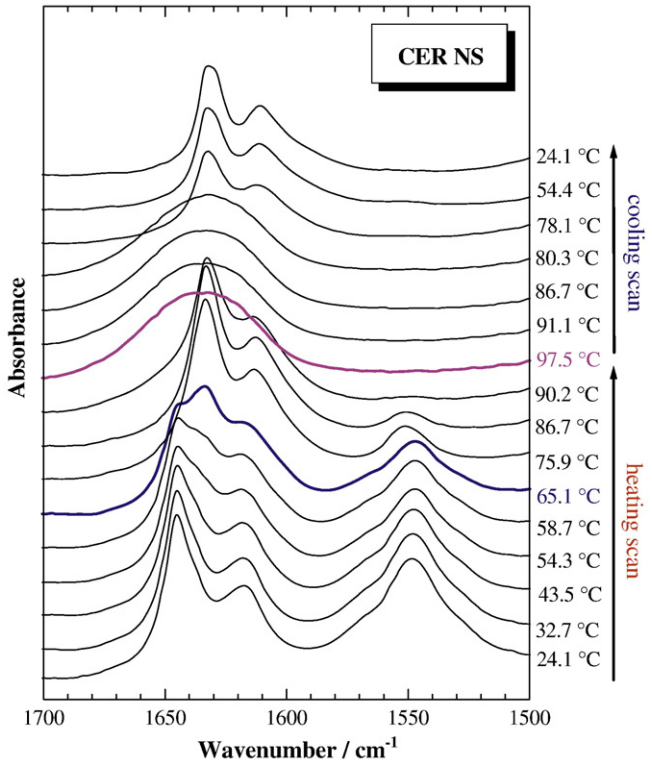

Fig. 6. Absorbance spectra of the 1700–1500 cm^{-1} spectral region of 1st heating and cooling scans of CER NS (10 mM phosphate buffer, 150 mM NaCl, 4 mM EDTA, in D_2O, pD 5.5). 1st heating scan: start at the bottom of the figure.

For illustrative purposes, the spectral region from 1700 to 1500 cm^{-1} of a ceramide film (CER NS) is shown in Fig. 6. At low temperature the amide I mode is split into a doublet (1645 and 1617 cm^{-1}), whereas the amide II is quite broad with its maxima located at ca. 1545 cm^{-1}. With increasing temperature strong alterations in the shape of the amide bands are observed. At ca. 66 °C the overall band shape of the amide I is shifted to lower wavenumbers (ca. 1630 cm^{-1}), indicating a re-organisation of the polar head groups. The shift to lower wavenumbers indicates a stronger involvement of the amide group in a hydrogen bond network. The organisational changes in the polar head group region correspond with the re-organisation of the hydrocarbon chain from an orthorhombic to a hexagonal chain packing (compare Figs. 3A, B and 6). It is to mention that there is also a frequency shift of the amide I to lower wavenumbers due to the fact that this mode is not a pure carbonyl stretching mode and therefore contains minor contributions from other internal coordinates (Table 1) that are sensitive to the hydrogen–deuterium exchange. This shift is small with ca. $\Delta\nu = 5$ cm^{-1}.

A further increase of the temperature above the main phase transition induces a strong broadening of the amide I with its maximum between 1640 and 1650 cm^{-1}. Cooling down the sample to room temperature shows the re-appearance of the doublet of the amide I, with the maxima shifted to lower wavenumbers (Fig. 6).

The analysis of the amide II (experiment performed in D_2O) allows the monitoring of water penetration into the polar interface. With increasing temperature the amide II band decreases and completely disappears at the onset of the chain melting. This is a general observation for ceramides that water penetration is extremely low [2,4,54] and only fully realised at the onset of hydrocarbon chain melting (for more details see [11,34,35,49,52,54]).

Thus the positions of the amide I and amide II are used as marker bands for understanding the organisation and interaction in the polar interface.

3.2. Hydrated ternary lipid mixtures composed of an equimolar ratio of a ceramide, perdeuterated palmitic acid (pd-PA) and cholesterol (Chol)

3.2.1. CER NS:pd-PA:Chol

Using one lipid with perdeuterated alkyl chains and one lipid with proteated alkyl chains allows the simultaneous and separate monitoring of the hydrocarbon chain organisation within the same experiment.

In a ternary, fully hydrated system the melting property of CER NS alkyl chains is shifted to lower temperature with a strong broadening of the phase transition (from 45 to 75 °C) (Fig. 7A). This indicates that the gel phase is destabilised by the presence of palmitic acid and cholesterol. Also the absolute position of the symmetric methylene stretching vibration, which is shifted by ca. 0.5 cm^{-1} to higher wavenumbers compared to pure CER NS, indicates a lower structural organisation. The CER NS chains, however adopt an orthorhombic chain packing at room temperature, and the collapse of the doublet to a single peak arises at the onset of the main phase transition at ca. 57 °C.

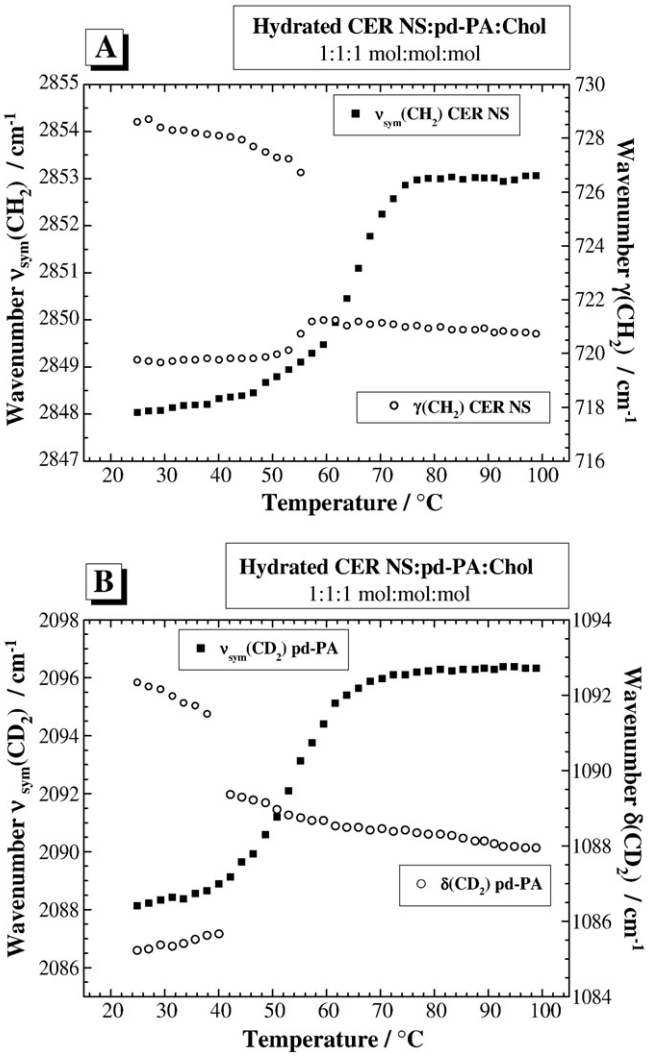

Fig. 7. Temperature dependence of (A) the symmetric CH_2 (methylene) stretching mode frequency ($\nu_{sym}(CH_2)$) and CH_2 (methylene) rocking mode frequency ($\gamma(CH_2)$) of hydrated CER NS and (B) the symmetric CD_2 (methylene) stretching mode frequency ($\nu_{sym}(CD_2)$) and CD_2 (methylene) scissoring mode frequency ($\delta(CD_2)$) of hydrated perdeuterated palmitic acid (pd-PA) of an equimolar mixture (1:1:1 mol:mol:mol) composed of CER NS, pd-PA and cholesterol (Chol). Buffer: 10 mM phosphate buffer, 150 mM NaCl, 4 mM EDTA, in D_2O, pD 5.5.

The hydrocarbon chains of palmitic acid (Fig. 7B) adopt also an orthorhombic packing at room temperature. This phase is stable up to 40 °C. The thermotropic response of the symmetric CD_2 stretching mode shows also a broad phase transition. Compared to pure pd-PA, the main phase transition is shifted by approximately 10 K to lower temperature. Thus at about 50 °C palmitic acid chains show a strong fluidisation, whereas the ceramide CER NS is still in its "crystalline-like" phase. At this temperature "crystalline-like" (gel-like) CER NS enriched domains are in equilibrium with molten palmitic acid enriched domains.

The data presented in Fig. 7 show strong evidence that both lipids are in fully extended *all-trans* conformation at skin physiological relevant temperature (30–35 °C).

Based on the melting properties of the two lipids, which are observed at 66 °C for CER NS and 52–54 °C for pd-PA, one could deduce that both lipids are organised in more or less separated domains. However, these domains are not formed of pure CER NS and pure pd-PA, respectively, because in both cases the thermotropic response of the lipids in the ternary systems is different to the response of the pure lipids. Furthermore, the phase cooperativity in the ternary system for both lipids is strongly reduced. Thus, it is very likely that these separated domains are enriched with cholesterol. This is also supported by the observation, that the orthorhombic crystalline phase of CER NS is stable up to 57 °C, whereas the orthorhombic phase of pd-PA collapses at much lower temperatures.

However, if one considers the onset and offset of the melting of the chains, the former is observed at ca. 40–45 °C and the latter at 65–75 °C, one has a broad temperature range where the two lipids melt. This observation may result from the fact that limited amounts of one lipid would mix with the other one. However, full mixing of both components is not obvious from the data.

The analysis of the interactions in the head group region of the pd-PA (Fig. 8) shows that the hydrogen bonding network is weakened at the onset of the main phase transition of the fatty acid. This can be deduced by a comparison of the initial position of the carbonyl stretch for palmitic acid in the ternary systems and pure palmitic acid (Figs. 5B and 8).

As shown in Fig. 9A, the amide I of CER NS is split into two components with their respective maxima at 1618 and 1644 cm^{-1}. A collapse to a single amide I peak is observed at ca. 59 °C, which corresponds to the onset of melting of the hydrocarbon chains of CER NS in the ternary mixture. The amide II (Fig. 9B) shows strong alterations at approximately 42 °C, and 59 °C. According to the thermotropic response of the hydrocarbon chains of CER NS, up to 50 °C the chains are packed in an orthorhombic lattice. However, a first alteration in the head group region of CER NS is observed at a temperature which corresponds to changes observed in the head group region of the fatty acid. So, does this indicate CER NS–pd-PA interactions or is it just coincidence? The amide I mode seems not to be sensitive to this alteration. With regard to water accessibility of the ternary lipid polar head group system, the H/D experiment (with D_2O) shows that the amide II completely disappears at the onset of the phase transition of the ceramide (data not shown). This behaviour is also observed for the other three systems.

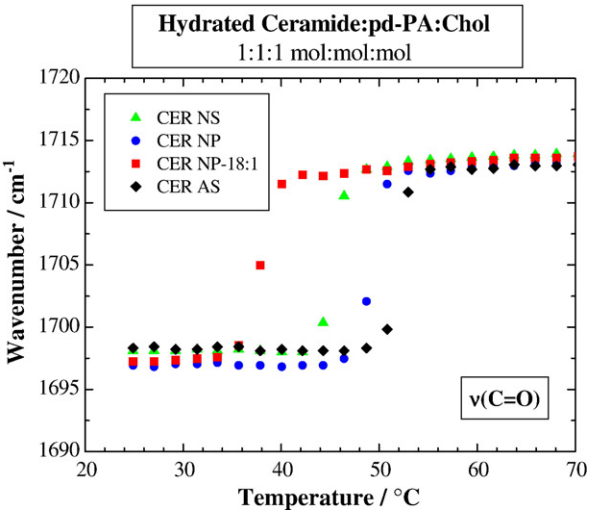

Fig. 8. Temperature dependence of the peak maximum of the ester carbonyl (ν(C=O)) of hydrated perdeuterated palmitic acid of an equimolar mixture (1:1:1 mol:mol:mol) composed of a ceramide, perdeuterated palmitic acid (pd-PA) and cholesterol (Chol) of 4 different ternary ceramide (CER NS, CER NP, CER NP-18:1 and CER AS) systems. Buffer: 10 mM phosphate buffer, 150 mM NaCl, 4 mM EDTA, in D_2O, pD 5.5.

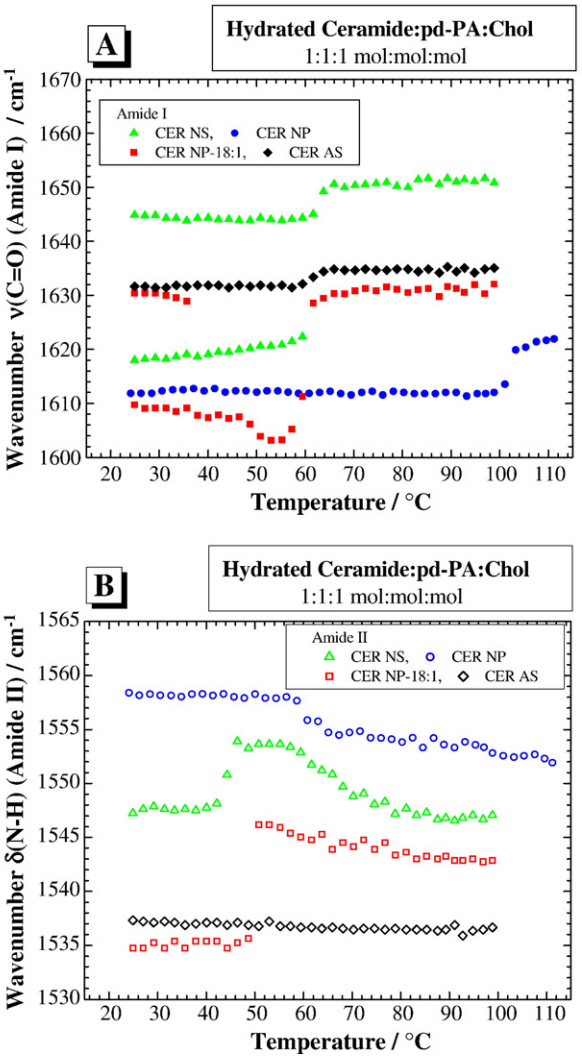

Fig. 9. Temperature dependence of the peak maximum/maxima of the (A) amide I and (B) amide II band of hydrated ceramides (CER NS, CER NP, CER NP-18:1 and CER AS) of an equimolar mixture (1:1:1 mol:mol:mol) composed of a ceramide, perdeuterated palmitic acid (pd-PA) and cholesterol (Chol). Buffer: 10 mM phosphate buffer, 150 mM NaCl, 4 mM EDTA, in H_2O, pH 5.5.

3.2.2. CER NP:pd-PA:Chol

Pure CER NP shows under fully hydrated conditions a gel to liquid-crystalline phase transition at 109 °C (Fig. 3A). In a ternary lipid system composed of an equimolar mixture with pd-PA and cholesterol, the melting temperature is reduced by 5 K. At room temperature the symmetric methylene stretching vibration of CER NP is shifted by ca. 0.5 cm^{-1} to higher wavenumbers, indicating a less tight packing

compared to the pure ceramide. The chains adopt a hexagonal chain packing (Fig. 10A). A chain packing in an orthorhombic lattice was not observed for the ternary, hydrated system, even after a storage of 4 weeks at 4, or 32 °C, respectively. In case the sample loses water, a re-crystallisation of the hydrocarbon chains into an orthorhombic lattice is induced.

The chain melting for the pd-PA alkyl chains seems to occur in two steps (Fig. 10B). A first increase of the $\nu_{sym}(CD_2)$ from 2088.7 to 2090.5 cm^{-1} is observed at ca. 45 °C and corresponds to the collapse of the $\gamma(CD_2)$ splitting. Thus below 45 °C the pd-PA acyl chains adopt an orthorhombic cell packing. A further increase of $\nu_{sym}(CD_2)$ from 2090.6 to 2096 cm^{-1} at ca. 63 °C is detected. This transition occurs in a similar temperature range as for the pure, hydrated pd-PA. At room temperature $\nu_{sym}(CD_2)$ of pd-PA in the ternary mixture is increased by 2.7 cm^{-1}, a strong evidence that the hydrocarbon chains of the fatty acid are less tightly packed compared to the pure fatty acid. In the ternary mixture both lipids show a chain melting close to the chain melting temperature of the pure systems. This would indicate that both lipids are organised in more or less pure domains. However, due to a broadening of the phase transition and to a slight decrease of the phase transition temperature for the lipids, and due to changes of the initial value of the wavenumbers of the methylene stretching vibration, a mixing with at least cholesterol has to be considered. Thus, this ternary system is prone for phase segregation.

The analysis of the carbonyl stretch of pd-PA (Fig. 8) shows a strong weakening of the hydrogen network at ca. 46 °C, which is consistent with a loosening of the orthorhombic chain packing and an increase of rotational freedom of the chains.

At room temperature the amide I of hydrated CER NP in the ternary mixture shows a band with a maximum located at 1613 cm^{-1}. Changes of the amide I of CER NP are observed as strong broadening above 100 °C with a shift to approximately 1621 cm^{-1}. For the amide II of CER NP in the ternary mixture a change is observed at 60 °C.

Water penetration arises at the onset of the CER NP phase transition.

3.2.3. CER NP-18:1:pd-PA:Chol

The synthetic ceramide CER NP-18:1 shows a strong depression of the main phase transition from 88 °C (pure CER NP-18:1) to 53 °C (ternary system) (Fig. 11A). The CER NP-18:1 acyl chains adopt a

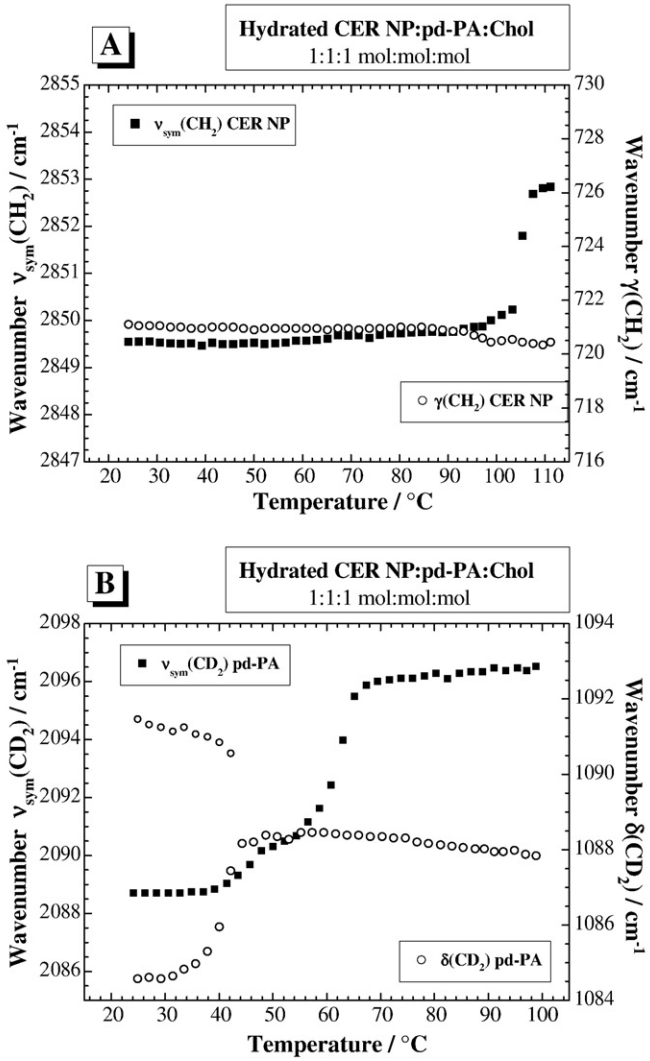

Fig. 10. Temperature dependence of (A) the symmetric CH_2 (methylene) stretching mode frequency ($\nu_{sym}(CH_2)$) and CH_2 (methylene) rocking mode frequency ($\gamma(CH_2)$) of hydrated CER NP and (B) the symmetric CD_2 (methylene) stretching mode frequency ($\nu_{sym}(CD_2)$) and CD_2 (methylene) scissoring mode frequency ($\delta(CD_2)$) of hydrated perdeuterated palmitic acid (pd-PA) of an equimolar mixture (1:1:1 mol:mol:mol) composed of CER NP, pd-PA and cholesterol (Chol). Buffer: 10 mM phosphate buffer, 150 mM NaCl, 4 mM EDTA, in D_2O, pD 5.5.

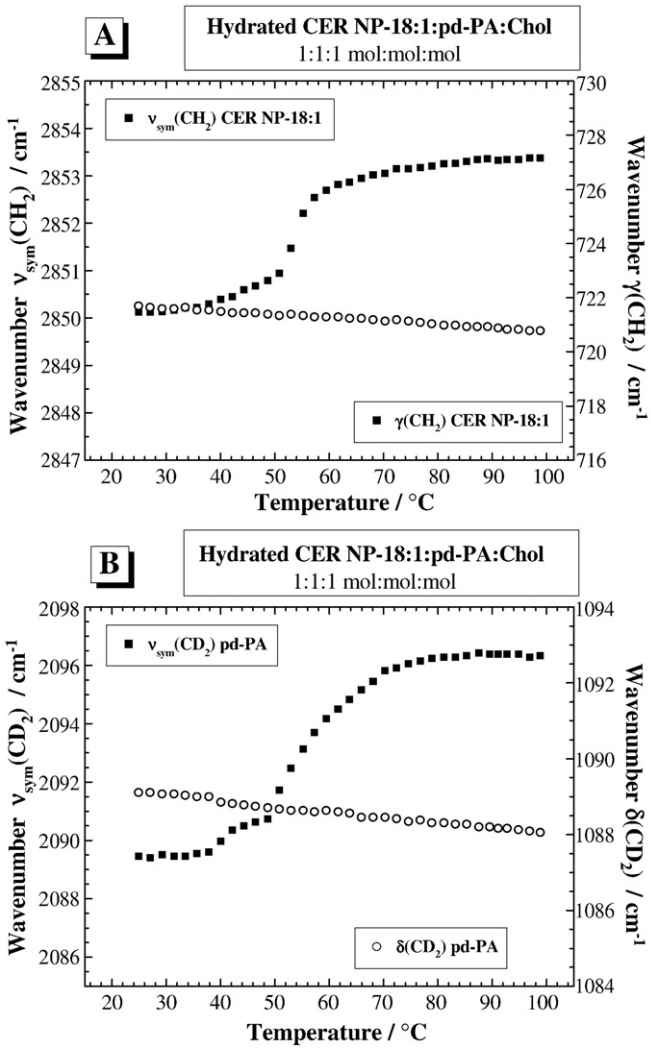

Fig. 11. Temperature dependence of (A) the symmetric CH_2 (methylene) stretching mode frequency ($\nu_{sym}(CH_2)$) and CH_2 (methylene) rocking mode frequency ($\gamma(CH_2)$) of hydrated CER NP-18:1 and (B) the symmetric CD_2 (methylene) stretching mode frequency ($\nu_{sym}(CD_2)$) and CD_2 (methylene) scissoring mode frequency ($\delta(CD_2)$) of hydrated perdeuterated palmitic acid (pd-PA) of an equimolar mixture (1:1:1 mol:mol:mol) composed of CER NP-18:1, pd-PA and cholesterol (Chol). Buffer: 10 mM phosphate buffer, 150 mM NaCl, 4 mM EDTA, in D_2O, pD 5.5.

hexagonal chain packing. Such a chain packing is also observed for pd-PA (Fig. 11B). The chain melting of the fatty acid arises as a two step melting. However, the average melting temperature is at ca. 55 °C. This behaviour would suggest mixing between both lipids and cholesterol.

The weakening of the fatty acid hydrogen network arises at 36–38 °C. At this temperature the amide I, which at room temperature is composed of a doublet (1610 and 1630 cm^{-1}), collapses to a single peak located at 1608 cm^{-1}. Between 50 and 60 °C strong changes of the position of the amide I are observed and above 60 °C the amide I band broadens and its maximum is shifted above 1630 cm^{-1}.

3.2.4. CER AS:pd-PA:Chol

The thermotropic response of CER AS in the ternary system shows a phase transition temperature at 62 °C (Fig. 12A). Compared to pure, hydrated CER AS the stability of the crystalline phase in the ternary system is reduced by approximately 16 K. The initial $\nu_{sym}(CH_2)$ is shifted by 0.5 cm^{-1} to higher wavenumbers for the CER AS acyl chains in the ternary system. The chains adopt an orthorhombic chain packing until the onset of the phase transition.

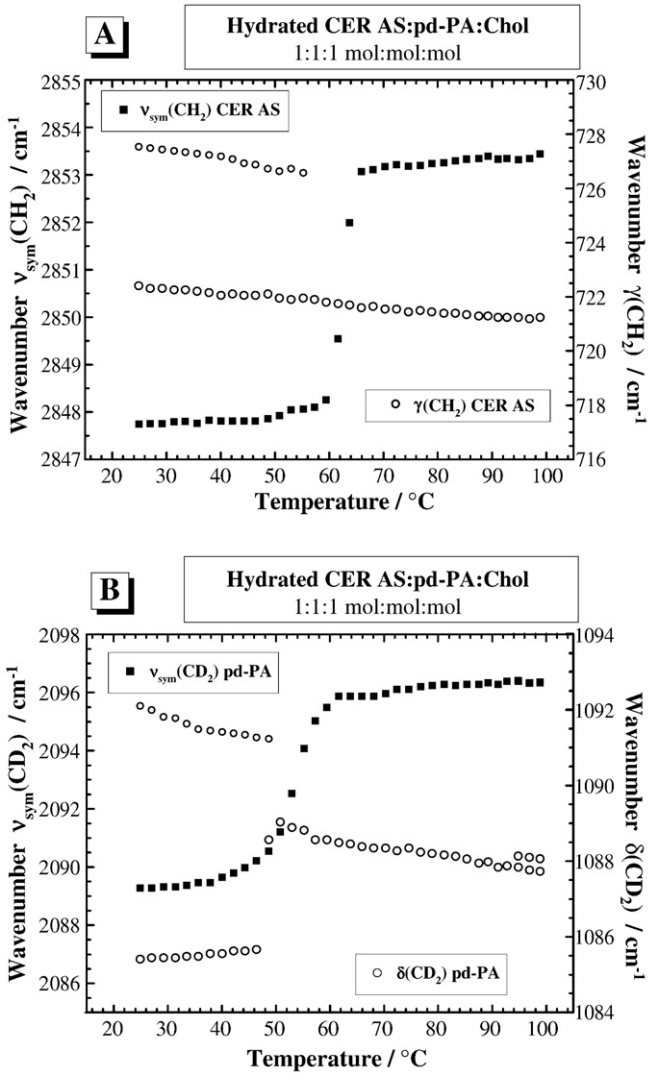

Fig. 12. Temperature dependence of (A) the symmetric CH_2 (methylene) stretching mode frequency ($\nu_{sym}(CH_2)$) and CH_2 (methylene) rocking mode frequency ($\gamma(CH_2)$) of hydrated CER AS and (B) the symmetric CD_2 (methylene) stretching mode frequency ($\nu_{sym}(CD_2)$) and CD_2 (methylene) scissoring mode frequency ($\delta(CD_2)$) of hydrated perdeuterated palmitic acid (pd-PA) of an equimolar mixture (1:1:1 mol:mol:mol) composed of CER AS, pd-PA and cholesterol (Chol). Buffer: 10 mM phosphate buffer, 150 mM NaCl, 4 mM EDTA, in D_2O, pD 5.5.

Perdeuterated palmitic acid shows its main phase transition at 53 °C, the temperature at which the orthorhombic chain packing collapses (Fig. 12B). The phase transition is broad, indicating a reduced cooperativity. This is in contrast to other studies [66]. In cases full water hydration is guaranteed, the phase transition of palmitic acid was always observed as a broad phase transition between 40 and 60 °C. Thus, pd-PA mixes at least with cholesterol.

At about 53 °C, the interactions in the head group of the fatty acid are strongly perturbed and reduced (Fig. 8). The position of the fatty acid carbonyl stretch (1698 cm^{-1}) shows that the fatty acid molecules are involved in a strong hydrogen bond network.

The maximum of the amide I is located at 1631 cm^{-1} and at 60 °C the amide I band is shifted to 1635 cm^{-1}, whereas the amide II, located at 1537 cm^{-1}, is more or less unaffected by temperature [66]. However, the position of the amide I and amide II are indicative for the involvement of the amide group in the formation of a strong hydrogen bond network. Full water hydration is observed at the onset of the CER AS phase transition.

4. Discussions

Compared to other lipids, like phospholipids, with a similar hydrocarbon chain length, hydrated ceramides exhibit extremely high gel to liquid-crystalline phase transition temperatures. Their hydrocarbon chains adopt orthorhombic chain packing [67–69]. This is the case for CER NS, CER NP and CER AS. These ceramides show a quite complex polymorphism with a solid–solid phase transition, which is marked by a transformation of an orthorhombic to hexagonal chain packing. This is consistent with published studies, whereas the extent of the formed phases is strongly sensitive to external parameters like hydration degree and storage temperature [34,49,52,58,66]. The hydrocarbon chains are tightly packed with the chains adopting *all-trans* conformation in a multilamellar layer. Various models were presented with regard to the orientation of the hydrocarbon chains [21,31,58,65]. Some of the models consider the hydrocarbon chains of the ceramide molecule being aligned parallel, whereas in other models a V-shaped structure is discussed (for more details see [21,58,59]).

The extent of this orthorhombic chain packing of ceramides depends, beside the chemical structure of the ceramide, also on parameters like temperature and the hydration degree [21,51,52].

The high phase transition temperature is due to strong interactions in the head group region between the hydroxyl groups and the amide group. The amide I of phytosphingosine ceramides are usually found at extremely low wavenumbers, in the region of 1610 cm^{-1} [65]. This is a clear indication of a strong involvement of the amide group in a tight hydrogen bond network. Higher amide I frequencies, as are found for sphingosine ceramides, are characteristic for weaker hydrogen bonding interactions between the head groups. Using the amide II shift in an H/D exchange experiment allows monitoring the water accessibility of the ceramide film. Hydration of a ceramide film is observed at the onset of the solid–solid transition, which corresponds to an orthorhombic to hexagonal chain packing transformation. The overall alignment of the hydrocarbon chains is also of importance. In a comparative study using phytosphingosine ceramides of type 3 of the same hydrocarbon chain length, but containing 2, 1 or no double bond, it was shown in a hydration experiment performed for 7 days at 37 °C that the ceramide with saturated hydrocarbon chains shows the lowest water penetration property, whereas the ceramide containing two double bonds exhibits the fastest hydration [54].

Full hydration is observed at the onset of the main phase transition. This is the case for the pure ceramides as well as for ceramides incorporated in a ternary system (see discussion below).

The mixing properties of ceramides with palmitic acid and cholesterol at an equimolar ratio are quite different depending on the considered ceramide (Table 2). In cases CER NP (hexagonal

Table 2
The characteristics of ceramides and palmitic acid in a hydrated ternary, equimolar mixture composed of ceramide, perdeuterated palmitic acid and cholesterol compared to the respective pure hydrated component. T_m: main phase transition temperature.

Characteristics	CER NS	CER NP	CER NP-18:1	CER AS
T_m of CER-ter[a] compared to pure CER	Decreased	Decreased	Decreased	Decreased
Chain ordering[b] CER-ter compared to pure CER	Decreased	Decreased	Decreased	Decreased
CER-ter acyl chain packing	Orthorhombic	Hexagonal	Hexagonal	Orthorhombic
Head group interactions[c] CER-ter compared to pure CER	Similar	Similar	Increased	Similar
T_m of pd-PA-ter[d] compared to pure pd-PA	Decreased	Similar	Decreased	Decreased
pd-PA-ter acyl chain packing	Orthorhombic	Orthorhombic	Hexagonal	Orthorhombic
Chain ordering[e] pd-PA-ter compared to pure pd-PA	Decreased	Decreased	Decreased	Decreased
Head group interactions[f] pd-PA-ter compared to pure pd-PA	Slightly increased	Slightly increased	Slightly increased	Slightly increased
Phase segregation	Yes	Yes	No	Yes

[a] Cer-ter: ceramide component in the ternary mixture composed of an equimolar ratio of ceramide, perdeuterated palmitic acid and cholesterol.
[b] Chain ordering derived from the absolute position (32 °C) of the symmetric stretching vibration of the ceramide.
[c] Head group interactions derived from the absolute position (32 °C) of the amide I stretching vibration of the ceramide.
[d] pd-PA-ter: perdeuterated palmitic acid component in the ternary mixture composed of an equimolar ratio of ceramide, perdeuterated palmitic acid and cholesterol.
[e] Chain ordering derived from the absolute position (32 °C) of the symmetric stretching vibration of the perdeuterated palmitic acid.
[f] Head group interactions derived from the absolute position (32 °C) of the carbonyl stretching vibration of the perdeuterated palmitic acid.

packing) is used, one observes that the presented data are indicative for phase segregation with palmitic acid (orthorhombic packing) at low temperature. Thus lipid domains are formed with more or less pure CER NP and palmitic acid. However, the palmitic acid domains are enriched with cholesterol. In cases a fatty acid component is used with longer chain length (stearic acid) the situation changes [70]. Both lipids (CER NP and stearic acid) adopt hexagonal chain packing and mixing becomes more likely. It is described that for the stearic acid ternary system, the melting property of the fatty acid is even reduced (main phase transition temperature is increased), an observation which deviates from the observation found for fatty acids of shorter chain length. This phenomenon is surprising because both components are hexagonally packed and up to now the melting temperature increase of stearic acid is not quite clear [70].

For the four investigated stratum corneum model systems, the thermotropic response of the palmitic acid chains are characteristic for a system being perturbed by another component, although reports have been presented showing for a ternary hydrated system composed of an equimolar mixture CER AS, palmitic acid and cholesterol a much higher cooperative melting for the fatty acid [66]. The melting of "pure" palmitic acid domains is not likely. In the case of the investigated ternary systems, cholesterol acts as a homogenising and fluidising agent. This has also been found by others [49].

The presented results also show that the hydrocarbon chains of the investigated sphingosine ceramide molecule adopt an orthorhombic cell lattice in the ternary system, which is consistent with the results of a study of a ternary system containing stearic acid [70]. This is however, not the case for the phytosphingosine ceramides, as is derived from the analysis of the methylene scissoring and/or rocking modes (Table 2).

Snyder et al. [71–75] have demonstrated that the quantitative evaluation of the splitting and broadening of the scissoring stretch band contour contains information to the extent of microaggregation, i.e. lateral domain formation, for lipids forming orthorhombic phases. The magnitude of the band splitting is a function of the domain size. Snyder et al. [71–73] have presented a relationship between the splitting of the scissoring band and the domain size, and found that their approach is most sensitive for domain sizes below hundred chains. This seems to be the case for the investigated ceramide ternary model systems which segregate (Table 2).

The difference between the mixing properties of CER NP and CER NP-18:1 with palmitic acid and cholesterol is quite remarkable, the former system showing phase segregation, whereas the second system is favouring the formation of a more or less "homogeneous" phase. The chemical nature of the polar head group as well as the hydrocarbon chain length of CER NP and CER NP-18:1 is the same. The difference results from the saturation degree of the hydrocarbon chain (Fig. 1). The presence of a double bond in the middle of the fatty acid ceramide hydrocarbon chain is responsible for a strong reduction of the crystallisation property of CER NP-18:1. For example, analysing the pure, hydrated ceramides, the initial position of the symmetric methylene stretch at 25 °C is $\nu_{sym}(CH_2) = 2848.9\ cm^{-1}$ for CER NP and $\nu_{sym}(CH_2) = 2849.6\ cm^{-1}$ for CER NP-18:1. This demonstrates a conformationally higher disorder for the hydrocarbon core of CER NP-18:1 compared to CER NP (Table 2). Furthermore, the hydrocarbon chains of CER NP-18:1 adopt a hexagonal chain packing, whereas pure CER NP is able to form an orthorhombic as well as hexagonal chain packing [54,65], in a ternary system the hexagonal packing is preferred. However, in the presence of stearic acid in hydrated ternary systems, CER NP adopts a hexagonal chain packing [70]. Thus, the presence of the free fatty acid has an impact on the packing property of the ceramide component.

For the ternary system, the hydrocarbon chains of both ceramides CER NP and CER NP-18:1 adopt hexagonal packing. Interestingly, also the hydrocarbon chains of palmitic acid in the CER NP-18:1, palmitic acid and cholesterol system is constrained to adopt hexagonal chain packing. This may favour mixing of both lipids.

The investigated sphingosine ceramides (CER NS and CER AS) show the formation of a "crystalline-like" phase with tightly packed and aligned hydrocarbon chains. The position of the initial symmetric methylene stretch at 25 °C for the pure ceramides is much below $\nu_{sym}(CH_2) = 2848\ cm^{-1}$. This is also the case for the ternary systems. Furthermore, orthorhombic chain packing determines the organisation of the hydrocarbon chains, although CER AS is also able to adopt its chains in a hexagonal lattice. This is due to the different nature of the head group structure, with CER AS having an additional hydroxyl group (in alpha position) compared to CER NS (Fig. 1). The presence of this additional hydroxyl group in the polar region alters the overall packing characteristics such that the hydrocarbon chains of CER AS are able to adopt both packing conformations. However, in the ternary system both ceramides adopt orthorhombic chain packing, as do the hydrocarbon chains of palmitic acid.

Comparing ceramides with the same chain length, or chain length distribution, one observed that the gel to liquid-crystalline phase transition is higher for the phytosphingosine (e.g. CER NP) compounds, in contrast to sphingosine ceramides (e.g. CER NS, CER AS). This may result from stronger interactions between the polar head groups. Monolayer measurements have revealed that the head group area of phytosphingosine is larger compared to sphingosine ceramides (unpublished results). This more open polar interface allows for phytosphingosine ceramides to form a stronger hydrogen bond network compared to sphingosine ceramides [65]. The low position of the amide I for CER NP compared to the other ceramides is an indication of a strong involvement of the amide group in a strong

hydrogen bond network. This is also observed for the ternary systems (Fig. 9A).

Thus, head group hydrogen bonding is less strong for sphingosines probably due to geometric constraints such that it allows the orthorhombic chain packing.

Therefore, variations in the head group architecture determine the formed phases. The extent of the formed phase can on the other side be modulated by the variation of the hydrocarbon chain configuration.

The observed phase transitions and chain arrangements have also been observed for isolated stratum corneum lipid extracts [36,76–78].

The macrostructure of the stratum corneum is represented by the bricks and mortar model (Fig. 13A) with the corneocytes (Fig. 13B) being the bricks of the wall [4]. Different models for the organisation of the stratum corneum lipids (Fig. 13C) have been presented [79–81]. Norlén [80] has proposed a few years ago, a skin barrier model for the stratum corneum, in which the intercellular lipids are organised in a single and coherent lamellar gel phase. The stabilisation of this membrane structure is due to the very particular lipid composition and lipid chain length distributions of the stratum corneum intercellular space and has virtually no phase boundaries. He also suggests that the intact, that means, the unperturbed, single and coherent lamellar gel phase is mainly located at the lower half of stratum corneum. In the upper stratum corneum layers, crystalline segregation and phase separation (Fig. 13C and D) may occur as a result of the desquamation process. Thus, Norlén differentiates between the microstructural arrangement of the upper and lower parts of the stratum corneum lipid barrier. As a consequence, the proposed stratum corneum lipid model shows a horizontal "phase separation", the upper layer being more heterogeneous in its structure, and the lower layer adopting a more or less homogeneous phase.

The single gel phase model is in opposition to the domain mosaic model (Fig. 13) which is formed of gel-like/crystalline-like domains delimitated from more or less liquid-crystalline-like phase boundaries (Fig. 13C and D), because the single gel phase model predicts a homogeneous lipid distribution so that phase separation is not observed, neither between liquid-crystalline and gel phases nor between different crystalline phases with hexagonal and orthorhombic chain packing, respectively (Fig. 13E).

3 years ago, Norlén [81] has also proposed that the skin barrier formation does not take place as a 'lamellar body' fusion process, but as a lamellar 'unfolding' of a small lattice parameter lipid 'phase' with cubic-like symmetry with subsequent 'crystallisation' and concomitant lamellar re-organisation of the extracellular lipid matrix.

In the same year, 2007, Norlén in collaboration with Plasencia et al. [82] have presented a biophysical study entitled "direct visualization of lipid domains in human skin stratum corneum's lipid membranes: effect of pH and temperature", showing that domain formation is observed for the stratum corneum lipid barrier. To "reconsolidate" the two models, the single gel phase model and the domain mosaic model, they investigated the impact of pH and temperature on the lipid organisation and found that these two parameters largely dominate the organisation of the lipids.

They concluded from their study [82]: "At skin physiological temperatures (28–32 °C), the phase state of these hydrated bilayers correspond microscopically (radial resolution limit 300 nm) to a single gel phase at pH 7, coexistence of different gel phases between pH 5 and 6, and no fluid phase at any pH. This observation suggests that the local pH in the stratum corneum may control the physical properties of the extracellular lipid matrix by regulating membrane lateral structure and stability."

Thus, both models seem to be of relevance. Another factor that has also to be carefully monitored is water hydration, as has been mentioned in this study.

Nevertheless, if one speculates a heterogeneous horizontal distribution of ceramides in the stratum corneum, one might be able to discuss such a "two-layered" model, because some ceramides are more prone for the formation of a more or less homogeneous phase, whereas other mixtures form phase separated domains.

This shows that the systematic investigations of the single components as well as lipid mixture systems are necessary to understand the quite complex nature of the microstructural organisation of the stratum corneum lipid barrier.

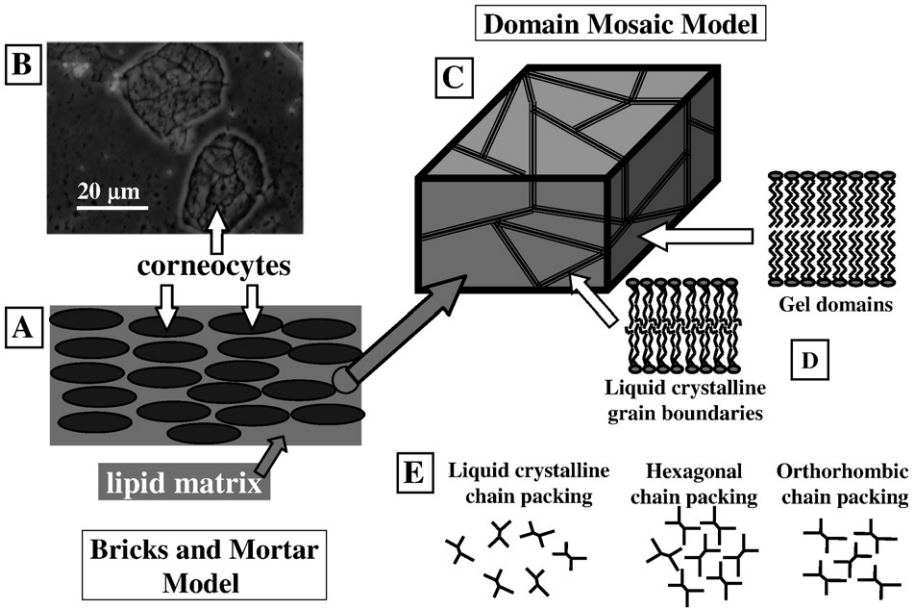

Fig. 13. Schematic representation of the stratum corneum and stratum corneum lipid structure. (A) "Bricks and mortar" model of the stratum corneum organisation. (B) Photomicrograph of isolated corneocytes. (C) Domain and mosaic model of the stratum corneum lipid barrier. (D) Gelphase lipids with hydrocarbon chains adopting an *all-trans* conformation and liquid-crystalline domains/grain boundaries with hydrocarbon chains adopting *gauche* conformations (microstructure of the stratum corneum lipid barrier). (E) Hydrocarbon chain packing.

5. Conclusions

When hydrated, in contrast to the two investigated sphingosine ceramides, the two analysed phytosphingosine ceramides in a ternary system composed of the ceramide, palmitic acid and cholesterol, exhibit hexagonal chain packing with extremely strong head group interactions via hydrogen bondings. Therefore, the driving force for microstructural arrangement of phytosphingosine ceramides results from the formed hydrogen bond network in the polar interface, i.e. the chemical structure of the head group. On the other side, the head group architecture of sphingosine ceramides mainly determines the organisation of the hydrocarbon chains, with favouring in general the orthorhombic perpendicular subcell lattice.

Based on the different chemical nature of ceramides the interaction and mixing properties with fatty acids and cholesterol are quite different. Phase segregated domains, with highly aligned hydrocarbon chains coexist with domains of higher conformational disorder. The extent of the microstructural organisation is governed by the chemical architecture and amount of the different ceramides. Also the presence of free fatty acid molecules modulates the phases adopted by the ceramide molecule and vice versa. Further modulation of the mixing property of the stratum corneum lipids may arise from external conditions like the presence of divalent cations, buffer components, pH, water hydration or the presence of extrinsic compounds. This has to be considered with more care in further studies.

The presented data support the domain mosaic model (Fig. 13), i.e. formation of distinct crystalline-like domains embedded in a more fluid phase, reflecting the properties of the stratum corneum lipid barrier. However, the generalisation of findings from the analysis of single systems, for other ceramides or other ceramide mixtures have to be considered with care, because the mixing properties seem to be modulated by a number of tiny factors like ceramide head group architecture, ceramide backbone and fatty acid chain composition, the presence and nature of the free fatty acid, cholesterol and derivatives thereof, as well as the external factors mentioned above.

Acknowledgments

This study was supported by the Deutsche Forschungsgemeinschaft (Germany). The ceramides were a gift from Cosmoferm and Goldschmidt AG, which is gratefully accredited.

References

[1] W. Montagna, W.C. Lobitz Jr. (Eds.), The Epidermis, Academic Press, New York, 1964.
[2] L.A. Goldsmith (Ed.), Physiology, Biochemistry, and Molecular Biology of the Skin, 2nd edition, Oxford University Press, New York, 1991.
[3] P. Elsner, E. Berardesca, H.I. Maibach (Eds.), Bioenginering of the Skin: Water and the Stratum Corneum, CRC Press, Boca Raton, 1994.
[4] R. Marks, J.L. Lévêque, R. Voegli, The Essential Stratum Corneum, Martin Dunitz Press, London, 2002.
[5] H. Schaefer, T.E. Redelmeier, Skin barrier, Principles of Percutaneous Absorption, S. Karger AG, Basel, 1996.
[6] P. Garidel, Mid-FTIR-microspectroscopy of stratum corneum single cells and stratum corneum tissue, Phys. Chem. Chem. Phys. 4 (2002) 5671–5677.
[7] P. Garidel, FTIR chemical mapping: a tool for spatially resolved characterisation of stratum corneum, in: R. Marks, J.L. Levêque, R. Voegli (Eds.), Stratum Corneum, Martin Dunitz Ltd, 2002, pp. 335–338, Chapter 52.
[8] B. Baroli, Penetration of nanoparticles and nanomaterials in the skin: fiction or reality, J. Pharm. Sci. 99 (2010) 21–50.
[9] P.W. Wertz, B. van den Bergh, The physical, chemical and functional properties of lipids in the skin and other biological barriers, Chem. Phys. Lipids 91 (1998) 85–93.
[10] K.C. Madison, D.C. Schwartzendruber, P.W. Wertz, D.T. Downing, Presence of intact intercellular lipid lamellae in the upper layers of the stratum corneum, J. Invest. Dermatol. 88 (1987) 714–718.
[11] P. Garidel, The thermotropic phase behaviour of phyto-ceramide 1 as investigated by ATR-FTIR and DSC, Phys. Chem. Chem. Phys. 4 (2002) 2714–2720.
[12] J.A. Bouwstra, G.S. Gooris, F.E.R. Dubbelaar, A.M. Weerheim, A.P. Ijzerman, M. Ponec, Role of ceramide 1 in the molecular organization of the stratum corneum lipids, J. Lipid Res. 39 (1998) 186–196.
[13] J.A. Bouwstra, G.S. Gooris, K. Cheng, A. Weerheim, W. Bras, M. Ponec, Phase behaviour of isolated skin lipids, J. Lipid Res. 37 (1996) 999–1011.
[14] M. Wegner, R. Neubert, W. Rettig, S. Wartewig, Structure of stratum corneum lipids characterised by FT-Raman spectroscopy and DSC, Int. J. Pharm. 81 (1996) R11–R14.
[15] S. Wartewig, R. Neubert, W. Rettig, K. Hesse, Structure of stratum corneum lipids characterised by FT-Raman spectroscopy and DSC. IV. Mixtures of ceramides and oleic acid, Chem. Phys. Lipids 91 (1998) 145–152.
[16] P. Garidel, A. Hauser, G. Förster, A. Blume, G. Rapp, N-Stearoyl-phytosphingosine lipid organisation as observed by synchrotron X-ray and atomic force microscopy, HASYLAB Annual Report 1, 2002, pp. 831–832.
[17] N. Ohta, S. Ban, H. Tanaka, S. Nakata, I. Hatta, Swelling of intercellular lipid lamellar structure with short repeat distance in hairless mouse stratum corneum as studied by X-ray diffraction, Chem. Phys. Lipids 123 (2003) 1–8.
[18] P.W. Wertz, M.C. Miethke, S.A. Long, J.S. Strauss, D.T. Downing, The composition of the ceramides from human stratum corneum and from comedones, J. Invest. Dermatol. 84 (1985) 410–412.
[19] M.A. Lampe, A.L. Burlingame, J. Whithney, M.I. Williams, B.E. Brown, E. Roitman, P. M. Elias, Human stratum corneum lipids: characterization and regional variations, J. Lipid Res. 24 (1983) 120–130.
[20] B. Glombitza, C.C. Müller-Goymann, Influence of different ceramides on the structure of in vitro model lipid systems of the stratum corneum lipid matrix, Chem. Phys. Lipids 117 (2002) 29–44.
[21] S. Wartewig, R.H.H. Neubert, Properties of ceramides and their impact on the stratum corneum structure: a review, Part 1, Skin Pharmacol. Physiol. 20 (2007) 220–229.
[22] S. Raudenkolb, S. Wartewig, G. Brezesinski, S. Funari, R.H.H. Neubert, Hydration properties of N-(α-hydroxyacyl)-sphingosine: X-ray powder diffraction and FT-Raman spectroscopic studies, Chem. Phys. Lipids 136 (2005) 13–22.
[23] S. Motta, M. Monti, S. Sesana, R. Caputo, S. Carelli, R. Ghindoni, Ceramide composition of the psoriatic scale, Biochim. Biophys. Acta 1182 (1993) 147–151.
[24] S. Motta, S. Sesana, R. Ghidoni, M. Monti, Content of the different lipid classes in psoriatic scale, Arch. Dermatol. Res. 287 (1995) 691–694.
[25] T. Dietz, U. Schick, K. Korevaar, Ceramide: natürlicher Schutz, der die Haut verjüngt, Sci. Newsl. Degusa 1 (2002) 5–8.
[26] E. Corbe, C. Laugel, N. Yagoubi, A. Baillet, Role of ceramide structure and its microenvironment on the conformational order of model stratum corneum lipids mixtures: an approach by FTIR spectroscopy, Chem. Phys. Lipids 146 (2007) 67–75.
[27] O. Bleck, D. Abeck, J. Ring, U. Hoppe, J.P. Vietzke, R. Wolber, O. Brandt, V. Schreiner, Two ceramide subfractions detectable in Cer(AS) position by HPTLC in skin surface lipids of non-lesional skin of atopic eczema, J. Invest. Dermatol. 113 (1999) 894–900.
[28] K.J. Robson, M.E. Stewart, S. Michelson, N.D. Lazo, D.T. Downing, 6-Hydroxy-4-sphingenine in human epidermal ceramides, J. Lipid Res. 35 (1994) 2060–2068.
[29] M. Ponec, A. Weerheim, J. Kempenaar, A.M. Mommaas, D.H. Nugteren, Lipid composition of cultured human keratinocytes in relation to their differentiation, J. Lipid Res. 29 (1988) 949–961.
[30] G.S.K. Pilgram, D.C.J. Vissers, H. Van Der Meulen, S. Pavel, S.P.M. Lavrijsen, J.A. Bouwstra, H.K. Koerten, Aberrant lipid organization in stratum corneum of patients with atopic dermatitis and lamellar ichthyosis, J. Invest. Dermatol. 117 (3) (2001) 710–717.
[31] D. Groen, G.S. Gooris, J.A. Bouwstra, New insights into the stratum corneum lipid organization by X-ray diffraction analysis, Biophys. J. 97 (2009) 2242–2249.
[32] M.W. de Jager, G.S. Gooris, I.P. Dolbnya, W. Bras, M. Ponec, J.A. Bouwstra, The phase behaviour of skin lipid mixtures based on synthetic ceramides, Chem. Phys. Lipids 124 (2003) 123–134.
[33] B. Ongpipattanakul, M.L. Francorur, R.O. Potts, Polymorphism in stratum corneum lipids, Biochim. Biophys. Acta 1190 (1994) 115–122.
[34] D.J. Moore, M.E. Rerek, R. Mendelsohn, Lipid domains and orthorhombic phases in model stratum corneum: evidence from Fourier transform infrared spectroscopy studies, Biochem. Biophys. Res. Commun. 231 (1997) 797–801.
[35] D.J. Moore, M.E. Rerek, R. Mendelsohn, Lipid domains and FTIR spectroscopy studies of the conformational order and phase behaviour of ceramides, J. Phys. Chem. B 101 (1997) 8933–8940.
[36] S. Zellmer, I. Zimmermann, C. Selle, B. Sternberg, W. Pohle, J. Lasch, Physico-chemical characterisation of human stratum corneum lipid liposomes, Chem. Phys. Lipids 94 (1998) 97–108.
[37] J. Kuntsche, H. Bunjes, A. Fahr, S. Pappinen, S. Rönkkö, M. Suhonen, A. Urtti, Interaction of lipid nanoparticles with human epidermis and an organotypic cell culture model, Int. J. Pharm. 354 (2008) 180–195.
[38] S. Pappinen, M. Hermansson, J. Kuntsche, P. Somerharju, P. Wertz, A. Urtti, M. Suhonen, Comparison of rat epidermal keratinocyte organotypic culture (ROC) with intact human skin: lipid composition and thermal phase behavior of the stratum corneum, Biochim. Biophys. Acta Biomembranes 1778 (2008) 824–834.
[39] H.H. Mantsch, D. Chapman, Infrared Spectroscopy of Biomolecules, Wiley-Liss, New York, 1996.
[40] B. Schrader (Ed.), Infrared and Raman Spectroscopy, VCH Weinheim, New York, Basel, 1995.
[41] P. Garidel, W. Hübner, A. Blume, A Fourier transform infrared spectroscopic study of the interaction of alkaline earth cations with the negatively charged phospholipid 1, 2-dimyristoyl-sn-glycero-3-phosphoglycerol (DMPG), Biochim. Biophys. Acta 1466 (2000) 245–259.
[42] N.B. Colthup, L.H. Daly, S.E. Wiberly, Introduction to Infrared and Raman Spectroscopy, Academic Press Ltd., London, UK, 1990.
[43] H. Günzler, H.M. Heise, IR-Spektroskopie. Eine Einführung, 3te Auflage, VCH-Verlag, Weinheim, 1996.

[44] D.C. Carrer, S. Härtel, H.L. Mónaco, B. Maggio, Ceramide modulates the lipid membrane organisation at molecular and supramolecular levels, Chem. Phys. Lipids 122 (2003) 147–152.
[45] S. Dikstein, A. Zlotogorski, Measurement of skin pH, Acta Dermatol. Venerol. (Stockh.) 185 (1994) 18–20.
[46] J. Ring, B. Eberlein-König, T. Schäfer, J. Huss-Marp, U. Darsow, M. Möhrenschlager, O. Herbert, D. Abeck, U. Krämer, H. Behrendt, Skin surface pH, stratum corneum hydration, trans-epidermal water loss and skin roughness related to atopic Eczema and skin dryness in a population of primary school children: clinical report, Acta Dermatol. Venerol. 80 (2000) 188–191.
[47] R. Winter, F. Noll, Methoden der Biophysikalischen Chemie, Teubner Studienbücher, Stuttgart, 1998.
[48] H.J. Galla, Spektroskopische Methoden in der Biochemie, Georg Thieme Verlag Stuttgart, 1988.
[49] M. Lafleur, Phase behaviour of model stratum corneum lipid mixtures: an infrared spectroscopy investigation, Can. J. Chem.—Revue canadienne de chimie 76 (1998) 1501–1511.
[50] K. Raith, H. Farwanah, S. Wartewig, R.H.H. Neubert, Progress in the analysis of stratum corneum ceramides, Eur. J. Lipid Sci. Technol. 106 (2004) 561–571.
[51] D. Kessner, A. Ruettinger, M.A. Kiselev, S. Wartewig, R.H.H. Neubert, Properties of ceramides and their impact on the stratum Corneum structure: a review, Part 2, Skin Pharmacol. Physiol. 21 (2008) 58–74.
[52] P. Garidel, Calorimetric and spectroscopic investigations of phytosphingosine ceramide membrane organization, Phys. Chem. Chem. Phys. 4 (2002) 1934–1942.
[53] P. Garidel, W. Richter, G. Rapp, A. Blume, Structural and morphological investigations of the formation of quasi-crystalline phases of 1,2-dimyristoyl-sn-glycero-3-phosphoglycerol (DMPG), Phys. Chem. Chem. Phys. 3 (2001) 1504–1513.
[54] P. Garidel, Structural organisation and phase behaviour of a stratum corneum lipid analogue: ceramide 3A, Phys. Chem. Chem. Phys. 8 (2006) 2265–2275.
[55] S.C. His, A.P. Tulleron, H.H. Mantsch, D.G. Cameron, A vibrational study of the CD_2 stretching bands of selectively deuterated palmitic and stearic acids, Chem. Phys. Lipids. 31 (1982) 97–103.
[56] S. Raudenkolb, W. Hübner, W. Rettig, S. Wartewig, R. Neubert, Polymorphism of ceramide 3. Part 1: an investigation focused on the head group of N-octadecanoylphytosphingosine, Chem. Phys. Lipids 123 (2003) 9–17.
[57] S. Raudenkolb, S. Wartewig, R. Neubert, Polymorphism of ceramide 3. Part 2: a vibrational spectroscopic and X-ray powder diffraction investigation of N-octadecanoyl phytosphingosine and the analogous specifically deuterated d35 derivative, Chem. Phys. Lipids 124 (2003) 89–101.
[58] P. Garidel, A. Hauser, G. Förster, A. Blume, G. Rapp, Aggregation behaviour of ceramide class 3 lipids, HASYLAB Annual Report 1, 2003, pp. 1009–1010.
[59] P. Garidel, A. Hauser, G. Förster, A. Blume, G. Rapp, The gel phase structure of hydrated ceramide 3b as investigated by synchrotron X-ray and atomic force microscopy, HASYLAB Annual Report 1, 2001, pp. 707–708.
[60] K. De Paepe, M.P. Derde, D. Roseeuw, V. Rogiers, Incorporation of ceramide 3B in dermatocosmetic emulsions: effect on the transepidermal water loss of sodium lauryl sulphate damaged skin, JEADV 14 (2000) 272–279.
[61] H. Lambers, W. Keuning, L.v.d. Heijden, W. van der Wilden, E. Brand, Ceramides, 1999, p. 1, Cosmoferm Report.
[62] F. Farin, H. Lambers, W. Keuning, W. van der Wilden, Human skin-identical ceramides, Cosmetics and Toiletries (1995) 126–132.
[63] Product data sheet of ceramide 3A, Degussa Goldschmidt Personal Care AG, reference B 03/01.
[64] P. Garidel, S.S. Funari, Molecular association of phytosphingosine ceramides of type III as investigated by synchrotron X-ray: Part 1, HASYLAB Annual Report 1, 2005, pp. 1053–1054.
[65] M.E. Rerek, H.C. Chen, B. Markovic, D. Van Wyck, P. Garidel, R. Mendelsohn, D.J. Moore, Phytosphingosine and sphingosine ceramide headgroup hydrogen bonding: structural insights through thermotropic hydrogen/deuterium exchange, J. Phys. Chem. B 105 (2001) 9355–9362.
[66] D.J. Moore, M.E. Rerek, R. Mendelsohn, Role of ceramides 2 and 5 in the structure of the stratum corneum lipid barrier, Int. J. Cosmetic Sci. 21 (1999) 353–368.
[67] P. Garidel, A. Hauser, G. Förster, A. Blume, G. Rapp, Insights into ceramide 3A molecular arrangement, HASYLAB Annual Report 1, 2004, pp. 801–802.
[68] J. Shah, J.M. Atienza, A.V. Rawlings, G.G. Shipley, Physical properties of ceramides: effect of fatty acid hydroxylation, J. Lipid Res. 36 (1995) 1945–1955.
[69] W. Abraham, D.T. Downing, Deuterium NMR investigation of polymorphism in stratum corneum lipids, Biochim. Biophys. Acta 1068 (1991) 189–194.
[70] M.E. Rerek, D. van Wyck, R. Mendelsohn, D.J. Moore, FTIR spectroscopic studies of lipid dynamics in phytosphingosine ceramide models of the stratum corneum lipid matrix, Chem. Phys. Lipids 134 (2005) 51–58.
[71] R.G. Snyder, M.C. Goh, V.J.P. Srivatsavoy, H.L. Strauss, D.L. Dorset, Measurement of the growth kinetics of microdomains in binary n-alkane solid solutions by infrared spectroscopy, J. Phys. Chem. 96 (1992) 10008–10019.
[72] R.G. Snyder, V.J.P. Srivatsavoy, D.A. Gates, H.L. Strauss, J.W. White, D.L. Dorset, Hydrogen/deuterium isotope effects on microphase separation in unstable crystalline mixtures of binary n-alkanes, J. Phys. Chem. 98 (1994) 674–684.
[73] R.G. Snyder, G. Conti, H.L. Strauss, D.L. Dorset, Thermally-induced mixing in partially microphase segregated binary n-alkane crystals, J. Phys. Chem. 97 (28) (2006) 7342–7350.
[74] R.G. Snyder, H.L. Strauss, D.A. Cates, Detection and measurement of microaggregation in binary mixtures of esters and of phospholipid dispersions, J. Phys. Chem. 99 (20) (1995) 8432–8439.
[75] D.J. Moore, R.G. Snyder, M.E. Rerek, R. Mendelsohn, Kinetics of membrane raft formation: fatty acid domains in stratum corneum lipid models, J. Phys. Chem. B 110 (2006) 2378–2386.
[76] J.A. Bouwstra, G.S. Gooris, F.E.R. Dubbelaar, M. Ponec, Phase behaviour of lipid mixtures based on human ceramides: coexistence of crystalline and liquid phases, J. Lipid Res. 42 (2001) 1759–1770.
[77] M. Janssens, G.S. Gooris, J.A. Bouwstra, Infrared spectroscopy studies of mixtures prepared with synthetic ceramides varying in head group architecture: coexistence of liquid and crystalline phases, Biochim. Biophys. Acta 1788 (2009) 732–742.
[78] J. Caussin, G.S. Gooris, M. Janssens, J.A. Bouwstra, Lipid organization in human and porcine stratum corneum differs widely, while lipid mixtures with porcine ceramides model human stratum corneum lipid organization very closely, Biochim. Biophys. Acta 1778 (2008) 1472–1482.
[79] B. Forslind, A domain mosaic model of the skin barrier, Acta Derm. Venerol. 74 (1994) 1–6.
[80] L. Norlén, Skin barrier structure and function: the single gel phase model, J. Invest. Dermatol. 117 (2001) 830–836.
[81] L. Norlén, Nanostructure of the stratum corneum extracellular lipid matrix as observed by cryo-electron microscopy of vitreous skin sections, Int. J. Cosmetic Sci. 29 (5) (2007) 335–352.
[82] I. Plasencia, L. Norlén, L.A. Bagatolli, Direct visualization of lipid domains in human skin stratum corneum's lipid membranes: effect of pH and temperature, Biophys J. 93 (2007) 3142–3155.